*Dental Traumatology* 2008; **24**: 177–182; doi: 10.1111/j.1600-9657.2007.00491.x

# Effect of different splint removal techniques on the surface roughness of human enamel: a three-dimensional optical profilometry analysis

**Zafer C. Cehreli[1], Manas Lakshmipathy[2], Ruya Yazici[3]**

[1]Department of Pediatric Dentistry, Faculty of Dentistry, Hacettepe University, Ankara, Turkey; [2]Zygo Corp., Middlefield, CT, USA; [3]Department of Conservative Dentistry, Faculty of Dentistry, Hacettepe University, Ankara, Turkey

Correspondence to: Zafer C. Cehreli DDS, PhD, Gazi M. Kemal Bulvari 61/11, 06570 Maltepe, Ankara, Turkey
Tel.: +90 312 3052289
Fax: +90 312 3243190
e-mail: zcehreli@yahoo.com

Accepted 18 January, 2006

**Abstract** – Because there is no standard protocol for the removal of resin-based materials that retain semi-rigid trauma splints on teeth, iatrogenic enamel damage caused by various splint removal techniques has remained unknown. The purpose of this study was to evaluate the effect of five different resin removal techniques (H6/H7 scaler, ultrafine diamond bur, ultrasonic scaler, 16-blade tungsten carbide bur, and Sof-Lex disks) on the surface roughness of human enamel. Three-dimensional white-light interferometry, a non-contact profilometry technique, was used to obtain qualitative and quantitative measurements of surface roughness both at baseline and after finishing procedures. Statistical analysis using Friedman test and Wilcoxon signed ranks test showed that the roughest enamel surface was obtained after splint removal with the hand scaler ($P < 0.05$). Overall, the smoothest enamel surface was obtained after removal of resin with Sof-Lex disks and the 16-blade tungsten carbide bur ($P < 0.05$).

Bonded semi-rigid splinting has been a common method for controlled passive mobilization of the traumatized tooth in various displacement and root fracture injuries. The bond between enamel and a splint-retaining resin is unique in dentistry in that, it is intended to be temporary. Immediately after completion of the splinting period, the splint and the bonding resin must be removed with minimum amount of trauma to the tooth. Accordingly, complete elimination of the adhesive resin attached to the enamel surface is mandatory to avoid prolonged accumulation of bacterial plaque (1) that may further lead to enamel decalcification and periodontal problems (2). The removal of the adhesive resin, however, can also cause a roughened enamel surface (3).

Because of their uneven geometry, removal of splint-retaining composite resins usually cannot be accomplished mechanically (i.e. with debonding pliers). Instead, the resin bulk needs to be reduced down to the enamel surface using several types of finishing burs or abrasive disks. At this point, the clinician may genuinely benefit from not 'debonding' a trauma splint, as debonding pliers have been shown to generate shearing forces that result in an irreversible damage to the enamel, ranging from microscopic fractures (4) to removal of a film of enamel from the tooth surface *in vivo* (5). On the other hand, complete reduction of the adhesive resin with rotary finishing instruments can also cause damage to the enamel surface; as without aid of strong magnification, it is virtually impossible to halt the removal process exactly at the enamel–resin interface. Surprisingly, no previous study has investigated the best technique for the removal of splint-retaining resins that would return the enamel as to near its original condition as possible while minimizing inherent enamel abrasion.

Removal of residual bonding resin and finishing of damaged enamel surface after orthodontic bracket debonding has been a subject of several research reports (3, 4, 6, 7). Commonly employed removal techniques include hand scalers (4, 8–10), rubber wheels and cups (8, 9), abrasive disks (7, 11), and assorted high- or low-speed burs (4, 10, 12). Ultrasonic removal techniques have also been studied (6, 13). Today, tungsten carbide finishing bur at low speed is most frequently recommended for removing residual orthodontic bonding materials (3, 14). It has been suggested that this technique provides easy and rapid removal of the bonding material and produces satisfactory surfaces without causing damage to enamel. Nevertheless, a recent study (11) has shown that debonded enamel samples displayed more enamel loss when polished with a slow-speed tungsten carbide bur, compared with an abrasive disk system (Sof-Lex). Interestingly, adhesive remnants were still observed microscopically on the enamel surface (11).

 

Overall, iatrogenic damage to enamel is an inevitable outcome of adhesive resin removal; regardless of the technique employed. At this point, the surface texture characteristics of such damaged surfaces appear to be a more critical factor to determine the long-term prognosis of enamel exposed to the oral environment. The purpose of this study was, therefore, to investigate the surface roughness and morphology of enamel after different splint-retaining resin removal techniques, using three-dimensional optical surface profilometry. The null hypothesis tested was that all tested finishing techniques would result in similar surface roughness values.

### Materials and methods

Non-carious human mandibular incisors, extracted for periodontal reasons, were used. All teeth were polished with a pumice and water mixture, rinsed and air-dried. The teeth were examined both under a stereomicroscope at 20× (Olympus, Tokyo, Japan) and by transillumination (Pluraflex HL 150; Litema GSD, Germany) to discard those with any visible structural defects, cracks or incipient lesions. Fifty sound teeth were selected in accordance with this protocol. Thereafter, the crowns were removed with a low-speed diamond disk under coolant water and embedded in self-curing acrylic resin, leaving the labial enamel surfaces exposed. In each specimen, the enamel surface was masked with a removable adhesive tape with a custom-made window that exposed a 2 × 3 mm enamel surface to serve both as a reference region for profilometry and as a standardized area for bonding and resin removal.

Before adhesive procedures, the specimen surfaces were initially analyzed with a three-dimensional surface profiler (NewView 5000; Zygo Corp., Middlefield, CT, USA) based on non-contact scanning white-light interferometry. Three-dimensional baseline interferograms of the specimens were recorded and the baseline values of four selected surface roughness parameters were obtained from linear profiles and calculated based on the equations presented in Fig. 1 for each specimen using image analysis software (MetroPro; Zygo Corp.). The measurements were made in triplicate along the long axis (central axis and 500 μm bilaterally) of each specimen and the mean value was recorded for each parameter. In the present study, the following surface roughness parameters were investigated (15, 16):

1. $R_a$ (average roughness): the Arithmetical mean deviation of all points from a plane fit to the test part surface.
2. $R_t$ (total roughness): the absolute value between highest and lowest peaks over the sample.
3. $R_{ku}$ (kurtosis): the measure of the randomness of heights, and of the 'sharpness' of a surface.
4. $R_{sk}$ (skewness): the measure of symmetry of the profile about the mean line. Negative skew indicates a predominance of valleys, whereas positive skew indicates a 'peaky' surface.

For bonding purposes, the exposed enamel surfaces were etched with 37% phosphoric acid for 15 s (17), rinsed with air–water spray for 10 s and air-dried. An acetone-based total-etch adhesive (Prime&Bond NT; DeTrey/Dentsply, Konstanz, Germany) was applied on the etched surfaces in accordance with the manufacturer's instructions. Thereafter, an approximately 2–2.5 mm-thick increment of light-cured resin composite (Spectrum TPH; DeTrey/Dentsply) was placed on the bonding area and light-cured for 40 s. The cured resin served as a representative composite bulk needed to retain a wire-type trauma splint. The adhesive tape was removed and the specimens were stored in deionized water at 37°C for 24 h. Thereafter, height of the composite bulk was reduced to approximately 0.5 mm, using a 8-blade tungsten carbide bur mounted on a high-speed handpiece under water cooling. The specimens were randomly distributed into the following groups for further removal of the residual splint adhesive attached to the enamel surfaces:

*Group 1*. The remaining adhesive was removed with a H6/H7 scaler (Hu-Friedy, Chicago, IL, USA).

*Group 2*. The remaining adhesive was removed with an ultrafine diamond finishing bur (No.17049; Diatech, Bern, Switzerland) with a high-speed handpiece, using water as the coolant.

*Group 3*. The remaining adhesive was removed with an ultrasonic scaler (Suprasson Pmax; Satelec, Merignac, France) under coolant water. A No.2 flat sickle tip was used.

*Group 4*. The remaining adhesive was removed with a 16-blade tungsten carbide bur (Komet H284; Brasseler Co., Lemgo, Germany) in a low-speed handpiece under coolant water.

*Group 5*. The remaining adhesive was removed with medium, fine and ultrafine aluminum oxide polishing disks (Sof-Lex; 3M, St Paul, MN, USA/Espe, Seefeld, Germany) in a low-speed handpiece under coolant water.

After finishing, the enamel surfaces were air-dried and inspected visually to ensure complete removal of the adhesive resin. In an attempt to simulate the clinical condition, the latter procedure was not performed under magnification. All removal procedures were performed by one calibrated operator to reduce variation of the force used on specimens. The Sof-Lex disks and the burs were changed after finishing of each sample, whereas the

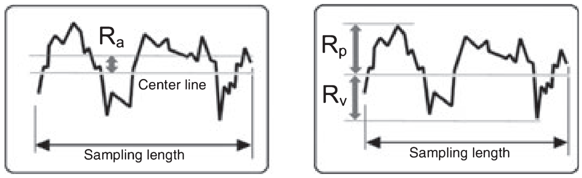


$$R_a = \frac{1}{L}\int_0^L |z(x)|dx \qquad R_t = R_p + R_v$$

$$R_{ku} = \frac{1}{n(R_q)^4}\sum_{i=1}^{i=n}(Y_i)^4 \qquad R_{sk} = \frac{1}{n(R_q)^3}\sum_{i=1}^{i=n}(Y_i)^3$$

*Fig. 1.* Equations used by image analysis software for calculation of the selected surface roughness parameters.

scaler and the ultrasonic scaler tips were changed after every two samples. The specimen surfaces were further subjected to non-contact scanning white-light interferometry to obtain post-treatment interferograms and surface roughness values. During the profilometry analysis, the system operator was blinded to treatment allocations.

Within each group, differences between the baseline and post-treatment surface roughness values were analyzed statistically using Wilcoxon signed ranks test with $P$-values $< 0.05$ considered significant. Statistical comparison for each surface roughness parameter between the test groups was performed with Friedman test and Wilcoxon signed ranks test at the same level of confidence.

## Results

The average roughness ($R_a$), total roughness ($R_t$), kurtosis ($R_{ku}$), and skewness ($R_{sk}$) values of the test groups are presented in Table 1 as mean ± SEM. Within each test group, splint removal with H6/H7 scaler, ultrasonic scaler, and tungsten carbide bur did not significantly change the $R_a$, $R_t$, $R_{ku}$, and $R_{sk}$ values of enamel surfaces (Wilcoxon signed ranks test, $P > 0.05$). Removal of splint material from the enamel surface with the ultrafine diamond bur (group 2) significantly increased total roughness ($R_t$, $P > 0.05$). On the other hand, the average surface roughness significantly decreased in the Sof-Lex group (group 5, $P < 0.05$). The Friedman test revealed significant differences between the average roughness ($R_a$) and the total roughness ($R_t$) of all test groups ($P < 0.05$). Accordingly, the average roughness values obtained with the tungsten carbide bur (group 4) and Sof-Lex disks (group 5) were significantly lower than that of the H6/H7 scaler (group 1, Wilcoxon signed ranks test, $P < 0.05$). As for total roughness values, tungsten carbide bur created a significantly less roughened surface than did the H6/H7 scaler ($P < 0.05$). Use of Sof-Lex disks significantly reduced the total roughness in comparison with the H6/H7 scaler, ultrafine diamond bur, and the ultrasonic scaler ($P < 0.05$), but did not differ significantly from that of the tungsten carbide bur ($P > 0.05$).

For the kurtosis and skewness parameters, there was no significant difference between any of the treatment groups (Friedman test, $P > 0.05$). Except enamel samples, in group 2 (ultrafine diamond bur), the enamel surface displayed a predominance of 'valleys' as evidenced by negative post-treatment skew values. Although not significantly different from their control values and those of other test groups, the use of H6/H7 scaler and tungsten carbide bur increased the skewness of enamel samples.

Overall, the smoothest enamel surface was obtained after removal of splint material with Sof-Lex disks and the 16-blade tungsten carbide bur. The roughest surface was obtained after splint removal with the H6/H7 scaler. Pre- and post-treatment three-dimensional oblique plots (interferograms) and vertical surface (solid) plots of each test group are presented in Figs 2–6.

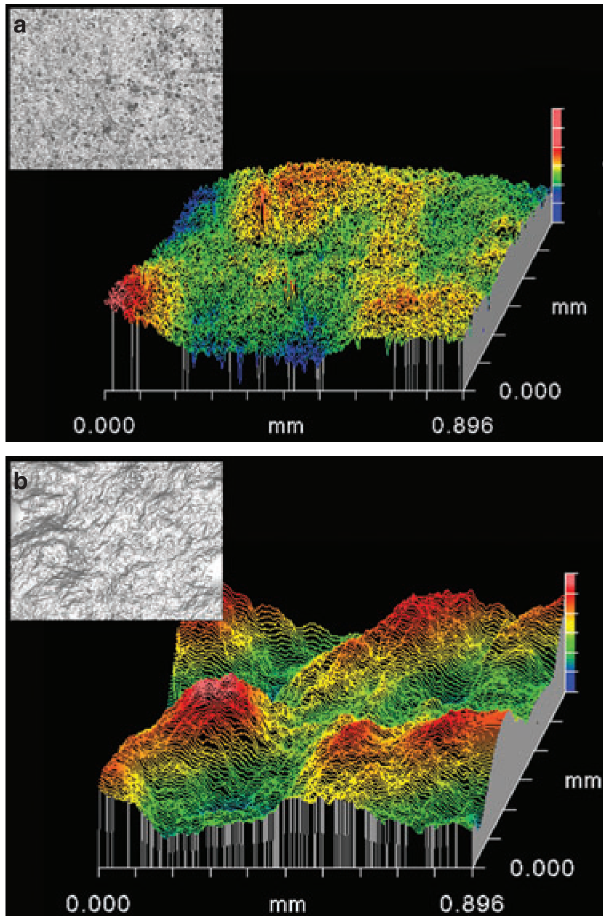


*Fig. 2.* Three-dimensional oblique surface plots (interferograms) of a representative specimen from group 1 (hand scaler): (a) pre-treatment plot and (b) post-treatment plot. On each figure, the solid plot (left upper corner) depicts the surface texture when viewed perpendicularly.

*Table 1.* Surface roughness values (mean ± SEM) of control and test specimens (in µm)

| Groups | Average roughness ($R_a$) | | Total roughness ($R_t$) | | Kurtosis (sharpness) ($R_{ku}$) | | Skewness ($R_{sk}$) | |
|---|---|---|---|---|---|---|---|---|
| | Control | Test | Control | Test | Control | Test | Control | Test |
| 1. Hand scaler | 3.4 ± 0.5 | 5.2 ± 0.9 | 40.6 ± 5.4 | 51.4 ± 6.8 | 4.7 ± 0.8 | 3.4 ± 0.3 | 4.8 ± 0.2 | –0.3 ± 9.8 |
| 2. Ultrafine diamond bur | 2.9 ± 1.0 | 3.2 ± 0.5 | 27.8 ± 3.6 | 35.9 ± 4.1 | 9.4 ± 3.6 | 6.3 ± 1.7 | 0.4 ± 0.4 | 0.14 ± 0.3 |
| 3. Ultrasonic scaler | 2.5 ± 0.5 | 4.2 ± 0.8 | 31.4 ± 4.7 | 41.7 ± 6.7 | 5.9 ± 1.1 | 4.24 ± 0.6 | –9.6 ± 0.3 | –5.6 ± 0.2 |
| 4. Tungsten carbide bur | 2.9 ± 0.7 | 2.5 ± 0.3 | 33.1 ± 4.8 | 30.5 ± 2.8 | 4.8 ± 0.8 | 4.16 ± 0.5 | –0.2 ± 0.1 | –8.1 ± 0.9 |
| 5. Sof-Lex disks | 4.6 ± 0.9 | 2.0 ± 0.4 | 38.5 ± 4.6 | 24.8 ± 2.6 | 3.9 ± 0.7 | 3.18 ± 1.0 | –4.2 ± 0.2 | –0.2 ± 0.1 |

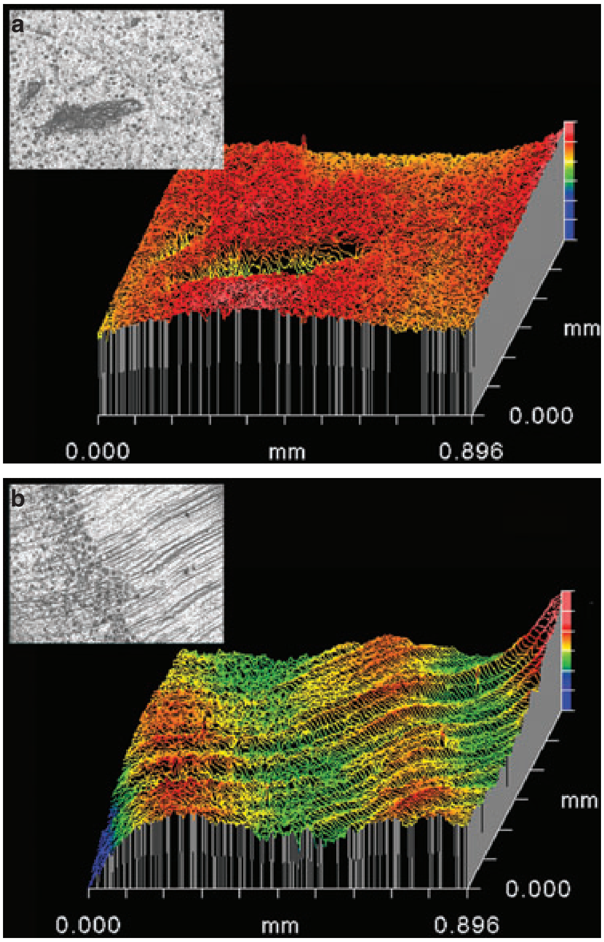


*Fig. 3.* Three-dimensional oblique surface plots (interferograms) of a representative specimen from group 2 (ultrafine diamond bur): (a) pre-treatment plot and (b) post-treatment plot. On each figure, the solid plot (left upper corner) depicts the surface texture when viewed perpendicularly.

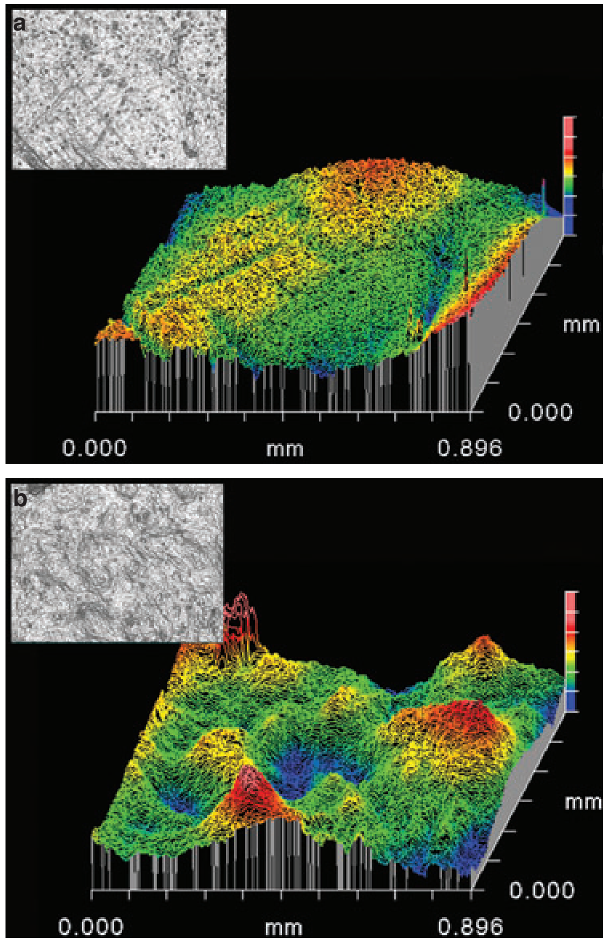


*Fig. 4.* Three-dimensional oblique surface plots (interferograms) of a representative specimen from group 3 (ultrasonic scaler): (a) pre-treatment plot and (b) post-treatment plot. On each figure, the solid plot (left upper corner) depicts the surface texture when viewed perpendicularly.

## Discussion

Three-dimensional surface profilometry is based on scanning white-light interferometry, which by splitting the incoming light, produces a light and dark fringe pattern (18). Together, a vertical scanning transducer and camera generate a three-dimensional interferogram of the surface processed by the computer and transformed by frequency domain analysis to give a quantitative non-contact three-dimensional image (Figs 2–6) (18, 19). After a profile is made, the computer analyses each pixel for its height data and the results are calculated based on the equation for each surface roughness parameter (15, 18). In the present study, the use of three-dimensional surface profilometry enabled visualization of the same enamel surface at both baseline and post-treatment stages, which would have been impossible by use of scanning electron microscopy because of the necessity of pre-treatment procedures (fixation and gold sputter-coating) which alter the sample surface. Moreover, the technique enables the sample surface to be studied more precisely (with more than 300 000 data points on an image with $640 \times 480$ pixel size) than a mechanical profilometer which, because of its stylus size, cannot penetrate certain microirregularities (19, 20).

From the results obtained herein, it was clear that the tested resin removal methods yielded different surface roughness values; necessitating rejection of the null hypothesis. The roughest surface was obtained after splint removal with the H6/H7 scaler (group 1). The representative interferogram of group 1 is clearly indicative of the 'valleys' produced by scratching the scaler over the enamel surface, contributing to the overall surface roughness (Fig. 2b). Nevertheless, the surface plot of the same surface also reveals distinct patterns of enamel detachment, suggesting that the shearing force generated by the scaler at the adhesive/enamel interface led to microcohesive fractures of the enamel, initially hybridized with the bonding resin (5). This phenomenon strongly resembles the fate of enamel after bracket debonding with pliers, where the partially decalcified enamel around the pores detaches more easily from the tooth surface and remains adhered to the bonding

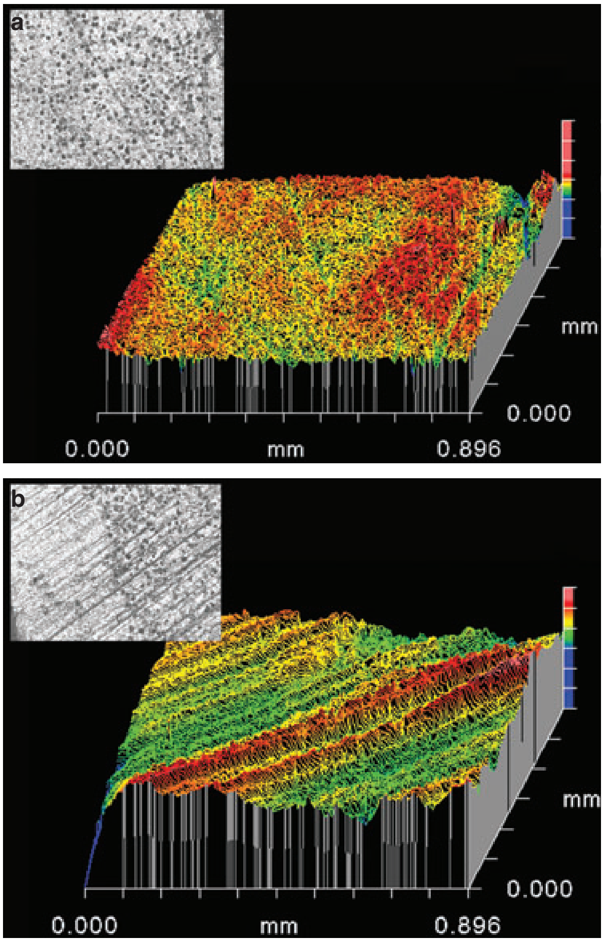


*Fig. 5.* Three-dimensional oblique surface plots (interferograms) of a representative specimen from group 4 (tungsten carbide bur): (a) pre-treatment plot and (b) post-treatment plot. On each figure, the solid plot (left upper corner) depicts the surface texture when viewed perpendicularly.

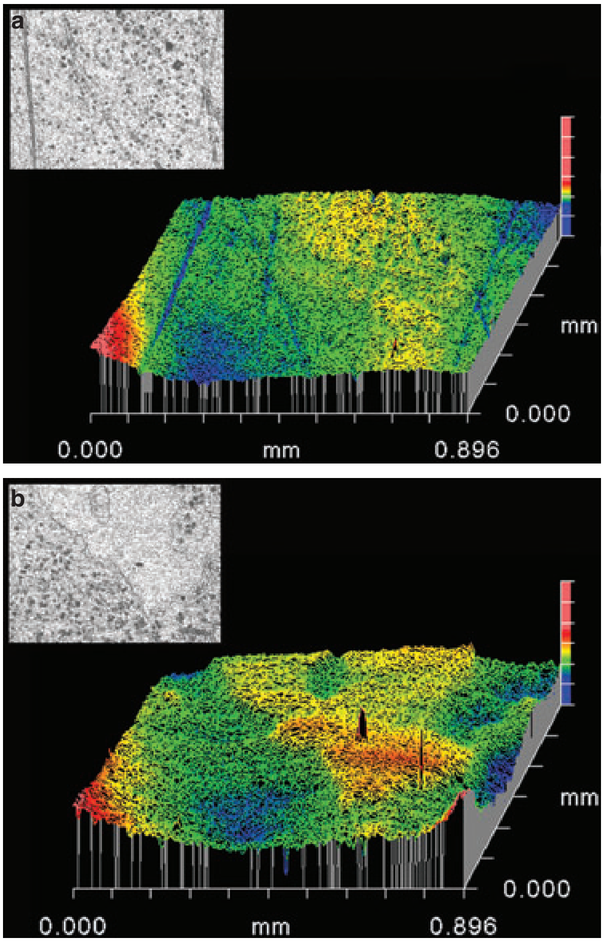


*Fig. 6.* Three-dimensional oblique surface plots (interferograms) of a representative specimen from group 5 (Sof-Lex disks): (a) pre-treatment plot and (b) post-treatment plot. On each figure, the solid plot (left upper corner) depicts the surface texture when viewed perpendicularly.

material during debonding (5, 7). To a lesser extent, a similar debonding effect was observed on the surface plot of the ultrasonic scaler group (Fig. 4b). This finding could be explained by a relatively lower shearing force needed to scale off the adhesive material with the ultrasonic handpiece, which resulted in a reduction of regions demonstrating cohesive fracture of the enamel. Based on these findings, regular or ultrasonic scalers, which apply a shearing force on the bonding resin, cannot be recommended for splint removal.

Because of its relatively weaker abrasive potential, the ultrafine diamond finishing bur was included in the study with anticipation of a smooth finish on enamel. Contrary, removal of splint material from the enamel surface with the ultrafine diamond bur (group 2) significantly increased the total roughness. This finding was supported with the interferogram and the solid plot of the enamel surface (Fig. 3b), revealing regular traces of the diamond bur in a wavy pattern. Rough surfaces promote plaque formation and maturation, and such high-energy surfaces (2) are known to collect more plaque, to bind the plaque more strongly and to select specific bacteria (1, 2). The use of ultrafine diamond bur, thus, cannot be recommended for splint removal.

In the present study, the 'smoothest' enamel surface was obtained after removal of splint material with Sof-Lex disks and the 16-blade tungsten carbide bur. However, these results must be interpreted with caution in that; both techniques altered the enamel surface from its natural state and that both methods, as with the other tested techniques, caused permanent damage to enamel. Although not significantly different, the post-treatment skewness value of enamel treated with Sof-Lex disks was lower than that of the tungsten carbide bur (Table 1). This finding was supported on the interferograms (Figs 5b and 6b) where the bur-cut enamel displayed uniform patterns of abrasion in contrast to a relatively smooth enamel surface in the Sof-Lex group. Polishing can be defined as the consistent abrasion of a surface with progressively finer materials. It is apparent that removal of the splint-retaining resin with a progressive-grit series of Sof-Lex disks resulted in a decrease of average surface roughness ($R_a$), at the expense of abrading enamel. Nevertheless, a recent study has shown that the mean volume of enamel removed by Sof-Lex disks is less than that removed by the tungsten carbide bur (11).

Although a comparison of surface roughness parameters with other studies has not been possible because of the lack of published data on the three-dimensional profilometry of enamel surfaces, the morphological findings obtained with the Sof-Lex disks and tungsten carbide burs corroborate with previous reports (4, 7, 10). Accordingly, Osorio et al. (7) and Retief & Denys (10) have shown that progressing down to an ultrafine Sof-Lex disk with water produced a similarly smooth enamel surface. On the other hand, results of the present study agree with others (4, 7) that the use of tungsten carbide burs is not necessarily the most effective procedure to produce a smooth enamel surface after removal of the adhesive resin. However, those studies did not employ quantitative analysis of the treated enamel surface, which showed herein that there was no significant difference in the overall surface roughness values between the Sof-Lex and the tungsten carbide bur treatment.

The present study provided detailed qualitative and quantitative data which can be extrapolated to the clinical practice. Further studies should include new polishing systems in order to complement the surface texture values obtained with Sof-Lex disks and tungsten carbide burs. However, based on the results obtained within the limitations of this study, the use of conventional scalers, diamond burs and ultrasonic handpieces cannot be recommended for the removal of composite resin.

#### Acknowledgements

The illustrations and formula presented in Fig. 1 are reprinted with permission from Zygo Corp. The primary author would like to express special thanks to Zygo Corp. for kindly granting permission for use of the three-dimensional optical profiler system mentioned in the text.

#### References

1. Quirynen M. The clinical meaning of the surface roughness and the surface-free energy of intra-oral hard substrata on the microbiology of the supra- and subgingival plaque: results of in vitro and in vivo experiments. J Dent 1994;22:S13–6.
2. Quirynen M, Bollen CML. The influence of surface roughness and surface-free energy on supra- and subgingival plaque formation in man. A review of the literature. J Clin Periodontol 1995;22:1–14.
3. Bishara SE, Trulove TS. Comparisons of different debonding techniques for ceramic brackets: an in vitro study. Part II. Findings and clinical implications. Am J Orthod Dentofac Orthop 1990;98:263–73.
4. Gwinnett AJ, Gorelick L. Microscopic evaluation of enamel after debonding: clinical application. Am J Orthod 1977;71:651–65.
5. Brosh T, Kaufman A, Balabanovsky A, Vardimon AD. In vivo debonding strength and enamel damage in two orthodontic debonding methods. J Biomech 2005;38:1107–13.
6. Krell KV, Courey JM, Bishara SE. Orthodontic bracket removal using conventional and ultrasonic debonding techniques, enamel loss and time requirements. Am J Orthod Dentofac Orthop 1993;103:258–66.
7. Osorio R, Toledano M, Garica-Godoy F. Enamel surface morphology after bracket debonding. J Dent Child 1998;65:313–7.
8. Pus MD, Way DC. Enamel loss due to orthodontic bonding with filled and unfilled resins using various clean-up techniques. Am J Orthod 1980;77:269–83.
9. Zachrisson BU, Arthur J. Enamel surface appearance after various debonding techniques. Am J Orthod 1979;75:121–37.
10. Retief DH, Denys FR. Finishing of enamel surfaces after debonding of orthodontic attachments. Angle Orthod 1979;49:1–10.
11. Tufekci E, Merill TE, Pintado MR, Beyer JP, Brantley WA. Enamel loss associated with orthodontic adhesive removal on teeth with white spot lesions: an in vitro study. Am J Orthod Dentofac Orthop 2004;125:733–40.
12. Rouleau BD, Marshall GW, Cooley RD. Enamel surface evaluations after clinical treatment and removal of orthodontic brackets. Am J Orthod 1982;81:423–6.
13. Jordan RD, Krell KV, Aquilino SA, Denehy GE, Svare CW, Thayer KE et al. Removal of acid-etched fixed partial dentures with modified ultrasonic scaler tips. J Am Dent Assoc 1986;112:505–7.
14. Howell S, Weekes WT. An electron microscopic evaluation of the enamel surface subsequent to various debonding procedures. Aust Dent J 1990;35:245–52.
15. Metropro surface texture parameters guide. CT, USA: Zygo Corp.; 2005.
16. Stout KJ, Sullivan PJ, Dong WP, Mainsah E, Luo N, Mathia T et al. The development of methods for the characterization of roughness on three dimensions. Luxembourg: Publication no. EUR 15178 EN of the Commission of the European Communities, 1994.
17. Kinch AP, Taylor H, Warltler R, Oliver RG, Newcombe RG. A clinical study of amount of adhesive remaining on enamel after debonding, comparing etching times of 15 and 60 seconds. Am J Orthod Dentofac Orthop 1989;95:415–21.
18. Marigo L, Rizzi M, La Torre G, Rumi G. 3-D profile analysis: different finishing methods for resin composites. Oper Dent 2001;26:562–8.
19. Joniot SB, Gregoire GL, Auther AM, Roques YM. Three-dimensional optical profilometry analysis of surface states obtained after finishing sequences for three composite resins. Oper Dent 2000;25:311–5.
20. Wassel RW, McCabe JF, Walls AW. Wear characteristics in a two-body wear test. Dent Mater 1994;10:269–74.